Unveiled the Source of the Structural Instability of HKUST-1 Powders upon Mechanical Compaction: Definition of a Fully Preserving Tableting Method

AUTHOR NAMES

A. Terracina[1,2], M. Todaro[1], M. Mazaj[3], S. Agnello[1], F. M. Gelardi[1], G. Buscarino[1,]*

AUTHOR ADDRESS

[1]Dipartimento di Fisica e Chimica, Università di Palermo, 90123 Palermo, Italy

[2]Dipartimento di Fisica e Astronomia, Università di Catania, 95123 Catania, Italy

[3]National Institute of Chemistry, Hajdrihova 19, 1000 Ljubljana, Slovenia

[*] Email:gianpiero.buscarino@unipa.it, web site: http://www.unipa.it/lamp/

ABSTRACT

Metal−organic frameworks (MOFs) are getting closer to finally being used in commercial applications. In order to maximize their packing density, mechanical strength, stability in reactive environments and many other properties, the compaction of MOFs powders is a fundamental step for the application field of research of these extraordinary materials. In particular, HKUST-1 is among the most promising and studied MOF. Contrary to what reported so far in literature, here we prove that the tableting of HKUST-1 powders without any damage of the lattice is possible and easy to get. For the first time, this kind of investigation has been performed exploiting its peculiar magnetic properties with the aid of the electron paramagnetic resonance spectroscopy. Indeed, they have allowed us to explore in detail all the smallest changes induced in the paramagnetic paddle-wheel units by application of the mechanical pressure on the material. This original approach has permitted us to unveil the main source of structural instability of HKUST-1 during compaction, i.e. the water molecules adsorbed by the powdered sample before tableting, and finally to establish a proper compaction protocol. Our conclusions are also fully supported by the results obtained with powder X-ray diffraction (XRD), Fourier-transform infrared spectroscopy (FTIR), thermogravimetric analysis (TGA), water sorption isotherms and surface area estimation with BET method, which prove that the tablet of HKUST-1 obtained by this new protocol actually preserves the crystal structure and porosity of the pristine powders. A morphological characterization has also been conducted with a combined use of optical and atomic force microscopies (AFM).

INTRODUCTION

In 2016, the first commercial application of Metal-Organic Frameworks (MOFs) technology was announced[1]. Since then, MOF research has reached a new development stage.[1] Among the thousands of different Metal-Organic Frameworks (MOFs) known today, one of the most interesting and now commercially available is HKUST-1. Thanks to its high surface area and large pore volume[2], HKUST-1 is a promising material for a wide range of applications, among which catalysis[3], drug delivery[4], gas storage and separation[5-11], are of major importance. Indeed, HKUST-1 can be used to purify hydrogen, methane, nitrogen or oxygen from carbon dioxide, contributing to decrease the greenhouse gases[12-14], or remove toxic gases as ammonia from contaminated air.[5-6] In the field of renewable energies, it can be used to store hydrogen or methane.[7-11] Before MOFs can be actually used for many of the described applications, a challenging obstacle have to be overcome. Indeed, nowadays, the conventional synthesis processes produce HKUST-1 (and MOFs in general) in the form of powder with low density. However, loose powders are generally technically not suitable for all those industrial applications, as they require high mechanical strength, large volumetric gas storage density and good stability in humid or reactive environments.[15-19] Furthermore, they are not even suitable for commercial applications because it is hard to handle them and their use can contaminate gas storage tanks.[20] For these reasons, several recent studies have been focused in the densification of many MOFs,[18-19,21-24] in the forms of tablets, monoliths, beads or thin film coatings,[25-29] in order to maximize the packing density and to overcome the above-mentioned technical problems, making the properties of MOFs closer to the industrial requirements. Relevant improvements for what concerns HKUST-1 tablets were actually verified in catalysis[22], mechanical stability[22], NH_3 removal capability[23], Xe/Kr selectivity[30] and HPLC separation of ethylbenzene and styrene[31]. However, a large number of experimental investigations reported in literature regarding HKUST-1 itself shows that the densification process usually affects negatively the porosity and the structure of the material.[21] Kim et al.[18] packed HKUST-1 in tablets pressed at 2.5 and 5 MPa. These samples showed a BET

surface area reduction of about 35% and 42%, respectively, compared with that of powder (1737 m^2/g). At pressure higher than 10 MPa, the authors also observed a partial collapse in the crystal structure.[18] The tablets of HKUST-1 prepared by Peterson et al.[23] with a pressure of 7 MPa and 70 MPa showed a BET surface area decrease of about 38% and 47%, respectively. More promising results were obtained by Dhainaut et al.[22] For a tablet pressed at 121 MPa, they observed a BET surface reduction of about 15% compared with that of their starting powder equal to 1288 m^2/g (a rather low value respect to those normally obtained for activated HKUST-1 powder). All these results indicate that compaction of powders induces structural damages in HKUST-1, generally reducing its main performances,[21] as for example water and CO_2 adsorption capacity.[18] The majority of the experimental investigations cited above was conducted through X-ray diffraction (XRD), scanning electron microscopy (SEM) images and gas isotherms for surface area determination with Brunauer–Emmett–Teller (BET) method. These techniques permitted a quantitative evaluation of the damage induced in HKUST-1 by application of mechanical pressure, but they do not provide detailed information of the effects on the structure of the network at a microscopic level. Furthermore, although the deleterious effects related to densification play an important role for HKUST-1 commercial applications, the processes responsible for the observed severe reduction of crystalline order have never been unveiled.

In the present paper, we show a way to compact HKUST-1 powders without ruining the material at all or worsening the quality of the material performances. The effect of the mechanical pressure has been investigated by conventional powder X-ray diffraction (XRD), nitrogen isotherms for surface area determination with BET method, Fourier-transform infrared spectroscopy (FTIR), thermogravimetric analysis (TGA), water sorption isotherms and combined optical/atomic force microscopy (AFM) for morphological characterization. Furthermore, in order to obtain new and more detailed information at the atomic scale level, the changes induced by compaction on the *magnetic properties* of HKUST-1 by electron paramagnetic resonance (EPR) spectroscopy were investigated

for the first time. These properties arise from the metal group of this MOF, which consists of a pair of Cu^{2+} ions (each with electronic spin S = 1/2) coordinated by four carboxylate bridges, to form a so-called paddle-wheel unit.[2] The carboxylate bridges are part of benzene 1,3,5-tricarboxylate linker molecules (BTC). The proper connection between metal groups and linkers generates a three-dimensional porous network with cubic symmetry ($[Cu_3(BTC)_2(H_2O)_3]_n$).[2] In addition to the structural bonds with carboxylate oxygen, each Cu^{2+} ion involves a fifth binding site that lies outside the plane identified by the O atoms of the carboxylic groups. Indeed, in as synthesized HKUST-1, this site is occupied by the oxygen of a molecule of crystallization water (i.e. incorporated during the synthesis of the material), whose desorption can be easily stimulated by a thermal treatment (activation process).[32] The two S=1/2 spins of Cu^{2+} ions are magnetically coupled through a super-exchange interaction which leads to an antiferromagnetic coupling.[33-34] The coupling constant of this interaction is about $|J| = 370\ cm^{-1}$, a rather large value that is essentially connected to the high geometric symmetry of the paddle-wheels.[32-33,35] As a consequence of this latter property, even small distortions of the crystalline structure of HKUST-1 are expected to considerably reduce this coupling. In this regard, EPR spectroscopy is a method very sensitive to the magnetic properties of the paddle-wheels, which in turn are very sensitive to the geometry of the site around the Cu^{2+} ions. For this reason, we have used EPR spectroscopy to investigate the changes occurring by compaction in the magnetic properties of HKUST-1. This original approach has allowed us to unveil many relevant information concerning the origin of the structural instability of HKUST-1 upon mechanical compaction and finally to develop a simple protocol of compaction, which allows to obtain mechanically stable tablets of highly packaged HKUST-1 powders with fully preserved crystalline structure and porosity.

MATERIALS AND METHODS

1. Materials and tablets preparation

HKUST-1 in powder form was purchased from Sigma-Aldrich and it was used in samples of about 150 mg. Before tableting, the powder was activated in an EPR glass tube. The activation process consisted in a heat treatment in air at 420 K for 1 hour. Then the powder was placed inside a pill maker under a hydraulic press. Each sample was pressed for 10 minute by applying a specific mechanical pressure. Two different pill makers and manometers were used (for pressure application and reading, respectively) depending on the range of pressure to be applied. In fact, for pressures from 0 to 30 MPa and for 40 MPa the circular sections of the pill makers were 0.5 cm^2 and 1.3 cm^2, respectively. The uncertainties in the corresponding pressures are about 3% and 10%, respectively. A set of samples was obtained, by using the following values of pressure: 1, 3, 10, 20, 30 or 40 MPa. In the following, all these samples will be referred to as "tablets", even if those obtained with values of pressure lower than 30 MPa were not found to form mechanically stable tablets (see Figure S1). After preparation, each tablet was crushed and put into an EPR tube that was then sealed. The samples were monitored by EPR spectroscopy for about 5 weeks after preparation. The following compact notation will be used in the present paper to indicate the various samples: "name-pressure-days after preparation", where "name" is a capital letter, which may be A or B. The letter A indicates that the sample was not heat treated after preparation of the tablet, inversely the letter B indicates that the sample was activated after two hours from the tableting. In the compact notation, "pressure" indicates the nominal pressure used to prepare the tablet, "days after preparation" indicates the time lapsed from the preparation of the tablet to the date of the measurements. In addition, two hydrated tablets were also produced. For the former tablet, before tableting at 40MPa, the powder was kept in air into a petri for 20 minutes (Powder H1), whereas for the second tablet, the parent powder was exposed to air moisture in a 1 cm diameter glass vial for about 2 hours (Powder H2). This latter method ensures a softer hydration process compared to that made with petri, as also confirmed by the fact that its color remains almost unchanged after 2 hours of exposition (see Figure S2). Hereafter we will refer

to these two last tablets with the name “H1-40MPa” and “H2-40MPa”, respectively. Both of them have been kept inside a sample holder which was sealed after tableting.

A sample of virgin activated HKUST-1 in powder form was also studied, for comparison, and hereafter it will be simply referred to as “Powder”. Finally, when a sample was reactivated the mark “-Reactivated” is added just at the end of its compact name. Tableting, aging and handling of both powder and tablet samples have been conducted in air at Relative Humidity (RH) of about 70%. A summary table of the main samples described here is present in the Supporting Information as Table S1.

2. EPR

EPR measurements were performed with a Bruker EMX micro spectrometer, working at a frequency of about 9.5 GHz (X-band). The magnetic-field modulation frequency was 100 kHz. The spectra were acquired by inserting the EPR glass tube containing the sample into a dewar flask. Only for measurement at 77 K, the dewar flask was filled with liquid nitrogen. All the spectra showed in the following were normalized for all the instrumental parameters and for the mass. The absolute concentrations of the paramagnetic centers present in the samples were estimated by comparing the double integrals of the EPR signals with that of a reference sample. The defects concentration in the reference sample was calculated using the instantaneous diffusion method in spin-echo decay measurements conducted in a pulsed EPR spectrometer.[36]

3. XRD

XRD measurements on powder and tablet samples were carried out using a PANalytical X’Pert PRO high-resolution diffractomer with CuKα1 radiation (λ = 1.5406 Å) in the range from 5 to 60° 2θ using step of 0.016° per 100 s at fully opened X’Celerator detector. Unit cell parameters fit was performed using Topas Academic v.6 software package (A. Coelho, Coelho Software, Brisbane, Australia, 2016).

4. N_2 isotherms

BET specific surface determination was based on a N_2 isothermal measurements at 77 K performed with a IMI-HTP manometric sorption analyzer (Hiden Isochema, Inc.). Before the measurements, the samples were outgassed at 420 K for 16 hours. The tablets were measured as-prepared, without any grinding.

5. AFM measurements

Atomic Force Microscopy (AFM) measurements were done in air by a Bruker FASTSCAN microscope working in soft tapping mode and using a FAST-SCAN-A probe (27 μm long triangular Silicon Nitride cantilever) with the following characteristics: 1400 kHz resonant frequency, 17 N/m force constant and about 5 nm apical radius. The size of the AFM images were 10μm x 10μm or 15μm x 15μm, depending on the local surface properties.

6. Thermogravimetry, IR measurements and water sorption isotherms

Thermogravimetry measurements were performed by a Q5000 IR apparatus (TA Instruments) under the nitrogen flow of 25 cm^3 min^{-1} for the sample and 10 cm^3 min^{-1} for the balance. The weight of each sample was ca. 3 mg. The experiments were carried out by heating the sample from room temperature to 650 °C with a rate of 10 °C min^{-1}. The temperature calibration was carried out using the Curie temperatures of standards (nickel, cobalt, and their alloys).

IR measurements were carried out with a Spectrum Two (Perkin Elmer) FTIR spectrometer with the resolution of 1 cm^{-1}.

Water sorption isotherms were measured using an IGA-100 gravimetric analyser (Hiden Isochema Ltd) at 25 °C in the relative pressure vapour range from 0.002 to 0.90. Before the measurements, samples were degassed at 150 °C for 12 hours.

RESULTS

1. Packing of HKUST-1 powder

The pictures of some of the tablets we have produced are reported in Figure S1. Only the tablets obtained with pressures of 30 MPa or higher were found to be self-standing. In Figure 1, the effective density (mass/volume of the tablet) measured after tableting as a function of the values of the pressure applied to the powder is reported. As shown, the density increases on increasing the applied pressure by following a sublinear dependence and it reaches a value of about 0.95±0.03 g/cm^3 for a pressure of 40 MPa. For sake of comparison, in Figure 1 we also indicate by red lines the calculated skeletal density of activated HKUST-1, 0.88 g/cm^3,[25] and that pertaining to the same system when it has adsorbed just one water molecule for Cu^{2+} site, 0.96 g/cm^3. This latter is a pertinent value of reference because the tableting process takes place in air and consequently we expect that a relevant fraction of the Cu site of the sample become actually saturated by a water molecule. As sown in Figure 1, the effective density estimated for the tablet obtained with a pressure of 40 MPa falls just between the two red lines, indicating an excellent volume packing of the powder. On the basis of this promising result, we have decided to investigate in more details the properties of the tablets of HKUST-1 obtained by using a mechanical pressure of about 40 MPa.

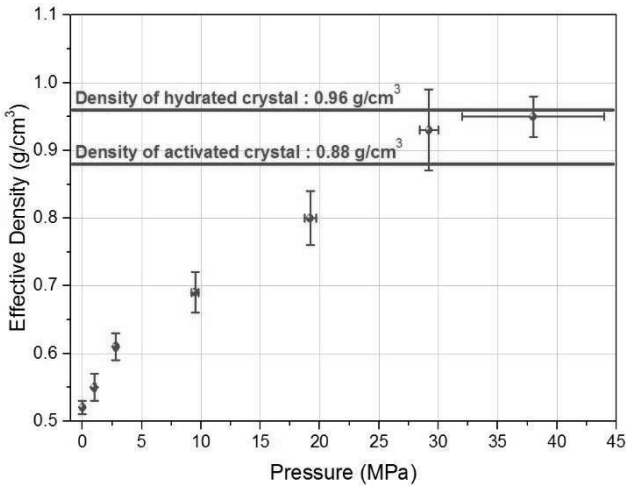

Figure 1. Effective density of tablets as a function of the applied pressure on HKUST-1 powder. The horizontal red lines indicate the calculated densities for activated HKUST-1 (0.88 g/cm^3) and for the same material after adsorption of just one water molecule for Cu^{2+} site (0.96 g/cm^3).[2]

2. Typical EPR spectra of HKUST-1 in powder form

EPR measurements of the Powder sample obtained at 77 K and 300 K are reported in Figure 2(a) and (b), respectively. The spectrum of Figure 2 (a) is characterized by a main resonance centered at B=325 mT with peak-to-peak width of about 37 mT and two smaller features at about B=12 mT and B=470 mT. The central resonance pertains to the complex involving a Cu^{2+} ion with electron spin S=1/2 coordinated with six water molecules, $[Cu(OH_2)_6]^{2+}$, and it is not connected to HKUST-1 framework.[33,37-39] Supposedly, it is a defect formed during the material synthesis.[33] A fine structure is also evident at about 325 mT comprising a multiplet of four lines, originating from the hyperfine interaction between the electron spin S=1/2 of the Cu^{2+} ion and its nuclear spin I_{Cu}=3/2.[33] The two smaller peaks (at about B=12 mT and B=470 mT) pertain to a triplet center (electron spin S=1) with axial symmetry, originating from the antiferromagnetic coupling between the two spin S=1/2 of the dimer of Cu^{2+} ions involved in each paddle-wheel.[33,37,40-42] In the spectrum of Figure 2(b) a large symmetric resonance is observed, centered at B=325 mT and peak-to-peak width of about 108 mT. In accordance with literature,[33] this resonance is ascribed to the triplet centers too. The appearance of a single symmetric line for such S=1 center, instead of the expected multi peak resonance, is due to the exchange interaction between the near magnetic paddle-wheels.[33] The strength of this interaction rises on increasing the temperature as a consequence of the population of the S=1 (triplet) state and it becomes significant above about T=160 K.[33]

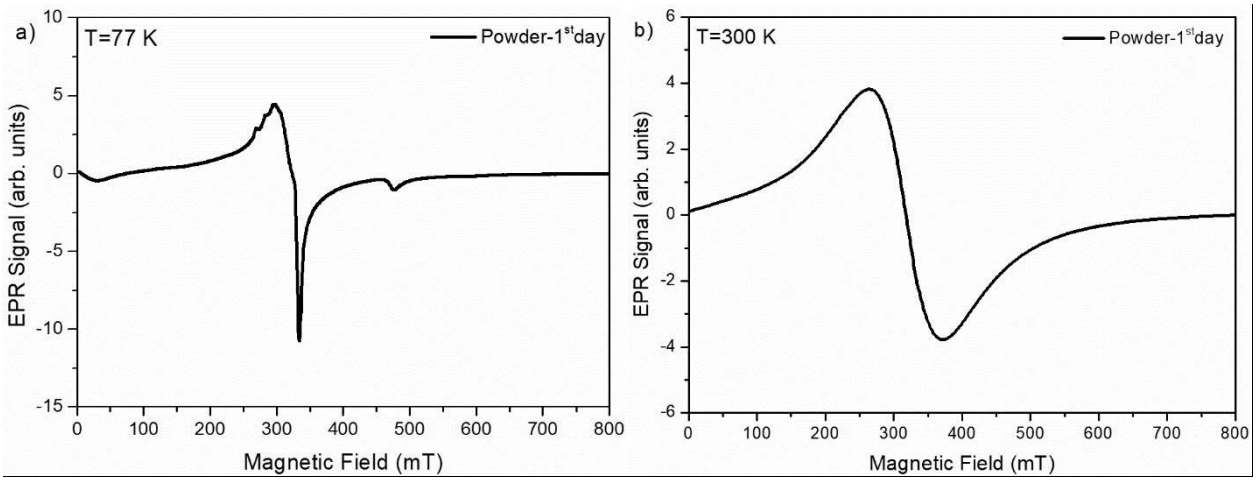

Figure 2. EPR spectra of the Powder sample obtained just after the activation and acquired at 77 K (a) and 300 K (b).

3. EPR spectra for H-type tablets of HKUST-1

EPR measurements of the tablet H1-40MPa obtained at 77 K and 300 K are reported in Figure 3(a) and (b), respectively. In order to recognize the effects of the various treatments considered, in Figure 3 we have also reported the spectra obtained for the same sample before exposure to air and tableting (Powder-1st day) and after hydration but before tableting (Hydrated Powder). The two graphs show that very relevant changes take place already when HKUST-1 powders are exposed to air. Indeed, at both temperatures, the hydrated powder shows the characteristic EPR spectrum of HKUST-1 severely damaged by hydrolysis.[39] Furthermore, Figure 3(a) and (b) reveal that the effect of compaction on such hydrolyzed powders is negligible, as the EPR spectra before and after preparation of the tablet are comparable.

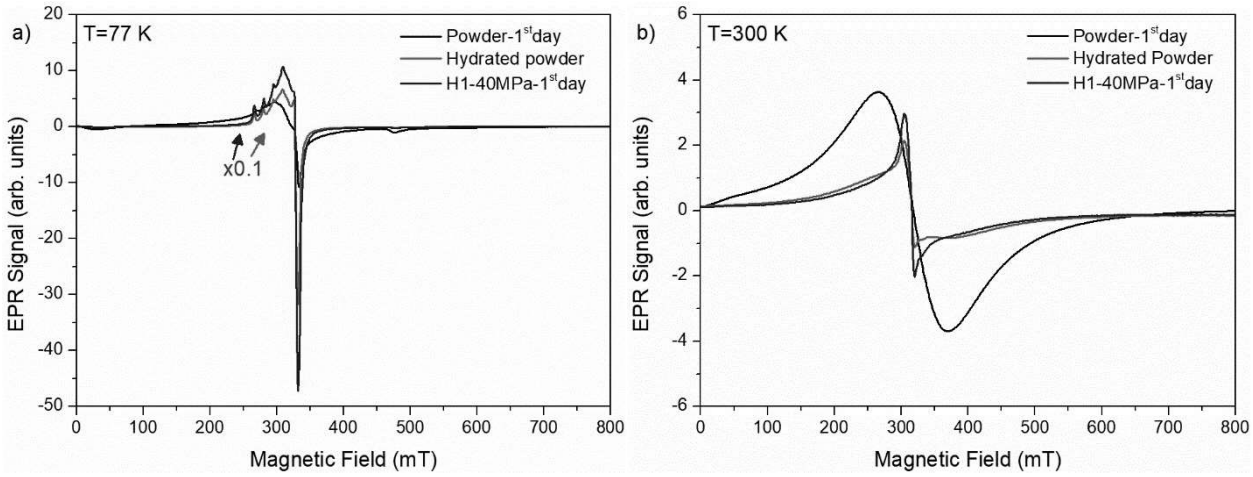

Figure 3. EPR spectra of the activated (black) and hydrated powders (pink) used to produce the 40MPa hydrated tablet (blue) acquired at 77 K (a) and 300 K (b).To make them easier to see, the spectra obtained at 77 K (except that of Powder) were multiplied by a factor of 0.1.

EPR measurements of the H2-40MPa obtained at 77 K and 300 K are reported in Figure 4(a) and (b), respectively. In this case, the spectra of the hydrated powder are very similar to that of the activated powder, in line with the less effective exposure to moisture of this sample with respect to the previous one H1-40MPa. We have noted just a reduction of the EPR signal acquired at T=300K (Figure 4b). However, it has been well established previously that this effect is reversible and inherently related to the hydration process of HKUST-1.[39] At variance, after compaction of the powders we have observed the growth of a very large contribution attributable to hydrolyzed paddle-wheels in the spectra acquired at T=77 K (main central resonance in Figure 4a).[39] These changes are less evident at T=300 K, presumably because they are mitigated by the inter-paddle-wheels exchange interaction which strongly affect the line shape of the resonance. In addition, we have observed a rapid evolution of the magnetic properties of the tablet as a function of time after preparation. This effect is shown in Figure 5 were for the same sample we have reported the comparison between the spectra acquired the day of the tableting and one week later. As shown, after just one week of storing of the sample in sealed glass tube, the signal attributed to hydrolyzed paddle-wheels increases by about a factor 5.

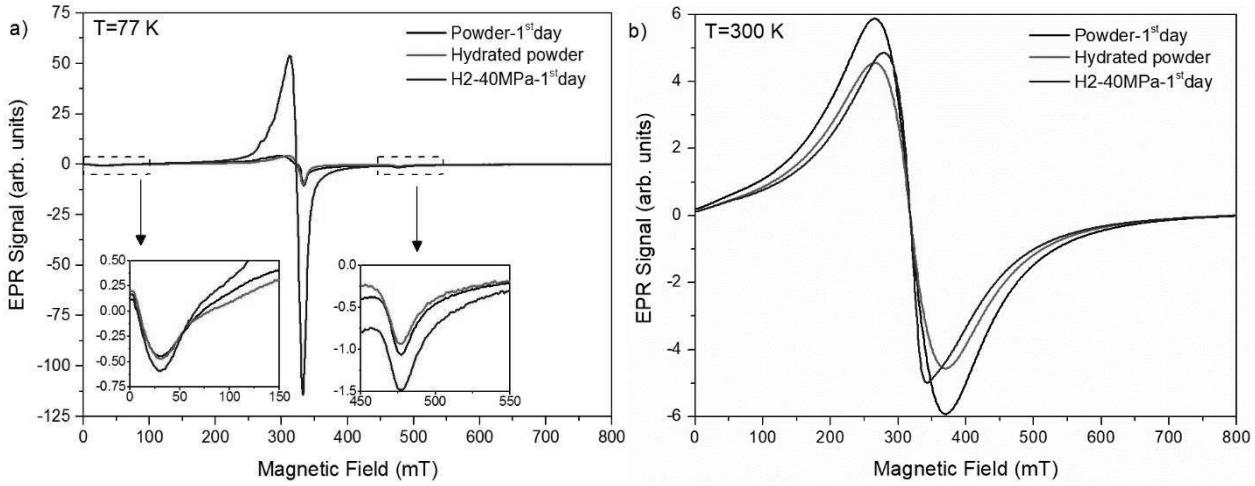

Figure 4. EPR spectra of the activated (black) and hydrated powders (pink) used to produce the H2-40MPa sample (blue) acquired at 77 K (a) and 300 K (b). The two insets in (a) show the zooms of the spectrum regions enclosed by the dashed panels.

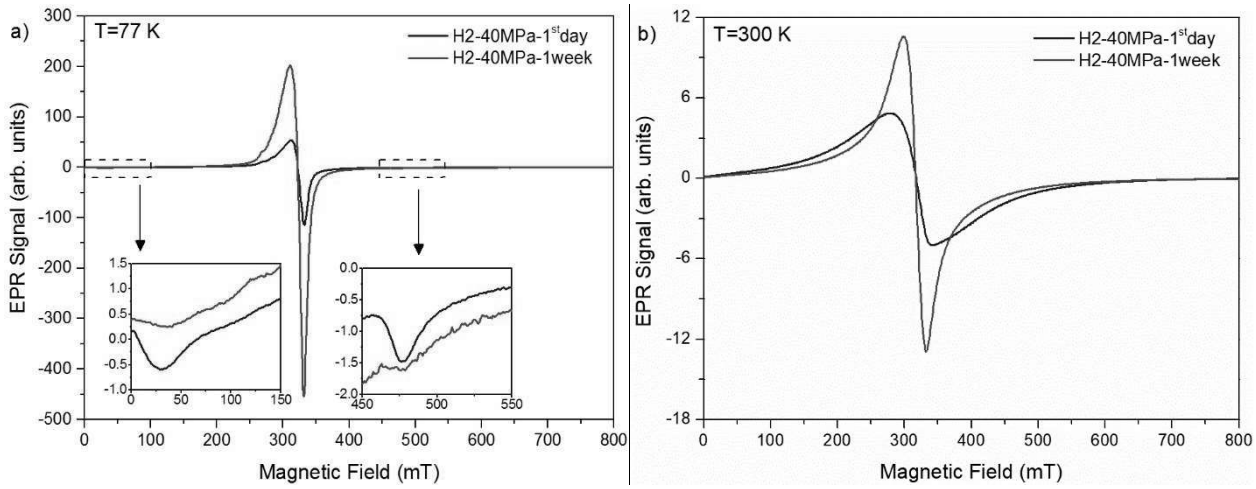

Figure 5. EPR spectra of the tablet H2-40MPa acquired at 77 K (a) and 300 K (b) the day of the tableting and one week after. The two insets in (a) show the zooms of the spectrum regions enclosed by the dashed panels.

4. EPR spectra for A- and B-type tablets of HKUST-1 at different pressures

EPR measurements of the most representative A-type tablets obtained at 77 K and 300 K are reported in Figure 6(a) and (b), respectively. In particular, by comparing the spectra acquired at 77 K, the principal difference concerns the intensity of the main resonance, which increases on increasing the pressure applied for the tableting of the sample. At variance, the spectra obtained at T=300 K present

less significant differences: it is possible to notice only a small narrowing of the line shapes on increasing the pressure, without detectable changes in intensity.

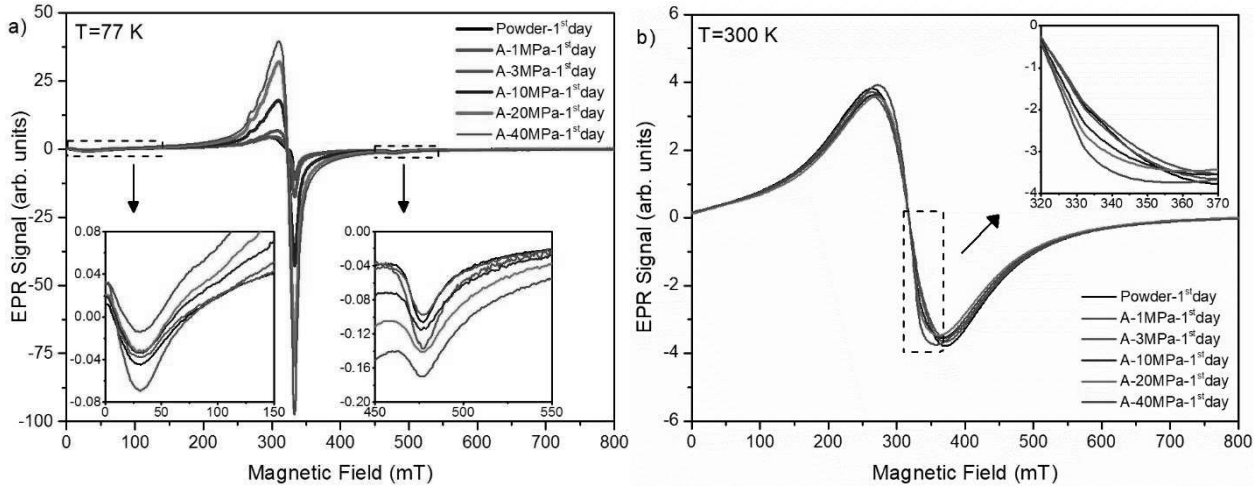

Figure 6. EPR spectra of some representative A-type tablets obtained just after tableting and of the Powder sample (in black), acquired at 77 K (a) and 300 K (b). The insets in both the graphs (a) and (b) show the zooms of the spectrum regions enclosed by the dashed panels.

As anticipated, B-type samples have been activated just after preparation of the tablets. In order to evaluate the effect of the thermal treatment, we have compared the EPR spectra obtained for the sample B-40MPa before and after activation. These data are shown in Figure 7(a) and (b) for 77 K and 300 K, respectively. For sake of comparison, the EPR spectra at both temperature of the Powder sample are also reported. Interestingly, the data reported in Figure 7 shows that the post-tableting activation induces a significant recovery of both the intensity and the lineshape of the central resonance.

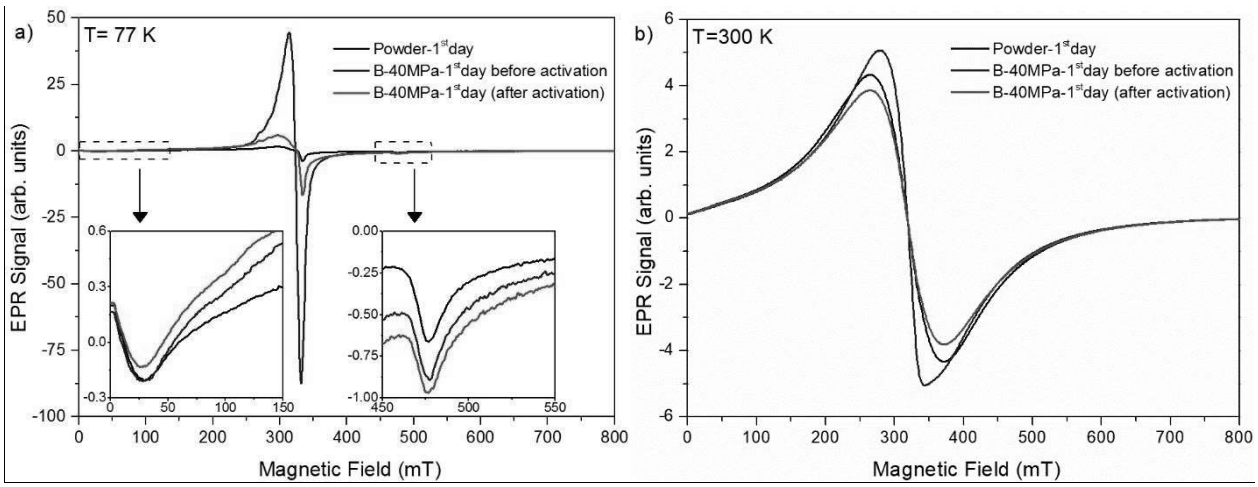

Figure 7. EPR spectra of the sample B-40MPa before activation and B-40MPa (after activation) obtained at 77 K (a) and 300 K (b). In black, the corresponding spectra of Powder-1stday are also shown for comparison. The two insets in (a) show the zooms of the spectrum regions enclosed by the dashed panels.

5. *Evolution of the EPR spectra for powder sample and for A-, and B-type tablets of HKUST-1 during the 5 weeks after activation and/or tableting*

EPR measurements of Powder sample acquired at different times after the first activation and obtained at 77 K and 300 K are reported in Figure 8(a) and (b), respectively. Figure 8(a) shows an increase of the amplitude of the main peak from the activation to 5 weeks later. In parallel, in Figure 8(b) we note a decrease of the amplitude of the central peak 5 weeks after the activation. No relevant change of the EPR lineshape is detected both at 77 K and 300 K. As already anticipated, both these effects are due to hydration and they have been observed and studied in depth by Todaro et al.[39] previously. It is also known that this stage of the process of hydration of HKUST-1 is totally reversible through an activation process (Figure S3).[39]

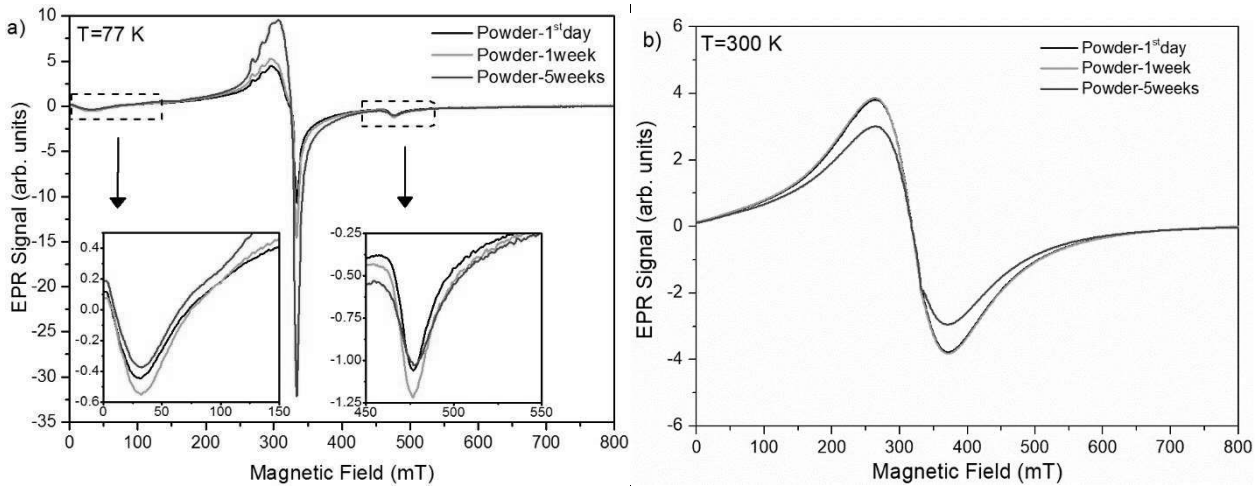

Figure 8. EPR spectra of the Powder sample acquired at different times after its first activation and obtained at 77 K (a) and 300 K (b). The two insets in (a) show the zooms of the spectrum regions enclosed by the dashed panels.

EPR spectra acquired for sample A-40MPa at 77 K and 300 K at different times after its tableting are shown in Figure 9(a) and (b) respectively, compared with those obtained for Powder-1stday at both temperatures. These measurements indicate that in the days following tableting, the EPR spectra undergo some relevant changes. In the spectra obtained at 77 K we observe the growth of new unknown spectral components peaked in the range of magnetic field from 60 mT to 150 mT (see the inset on the left in Figure 9(a)), whereas at room temperature a significant change of the lineshape is easily recognizable. These changes indicate that a relevant fraction of the paddle-wheels of the material become significantly distorted during the 5 weeks after preparation of the tablet.

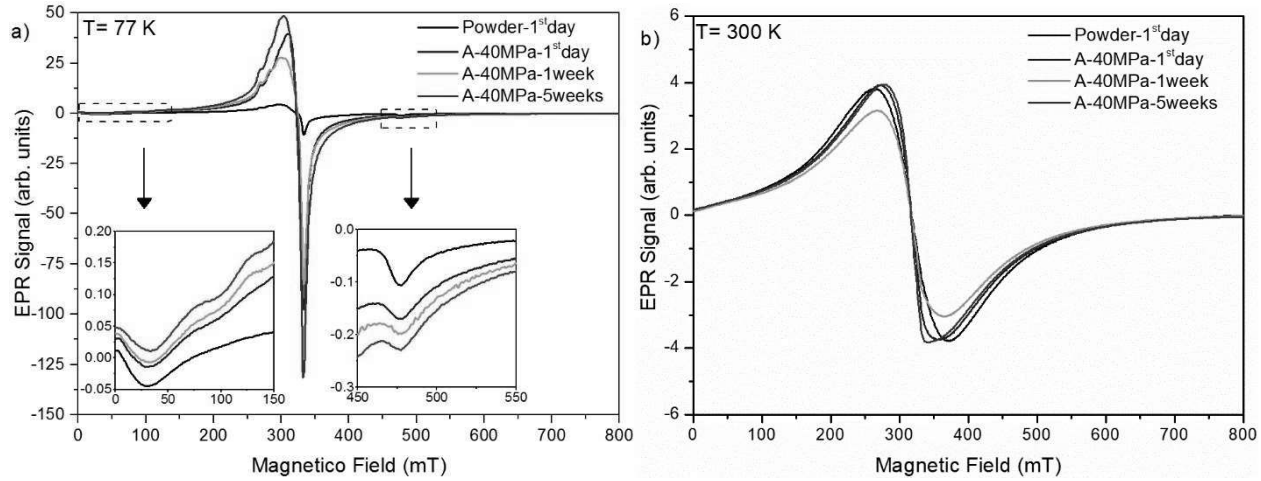

Figure 9. EPR spectra of the sample A-40MPa acquired at different time after its tableting and obtained at 77 K (a) and 300 K (b). In black, the corresponding spectra of Powder-1stday are also shown for comparison. The two insets in (a) show the zooms of the spectrum regions enclosed by the dashed panels.

Figure 10 shows EPR measurements obtained at 77 K (a) and 300 K (b) for the B-40MPa immediately after reactivation and 5 weeks after it, compared with those obtained for Powder-1stday. At both temperatures, we have observed very negligible variations of intensity and line shape. Therefore, from the point of view of its magnetic properties, the sample B-40MPa is a tablet which preserves almost unchanged the pristine properties of the material stably in time.

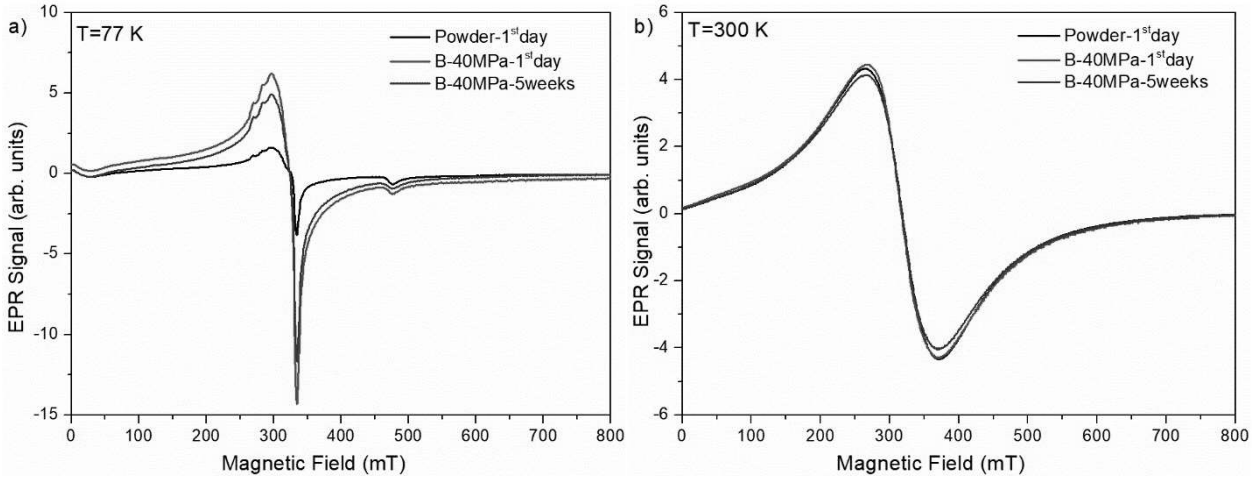

Figure 10. EPR spectra of the sample B-40MPa at the day of reactivation process and 5 weeks later, obtained at 77 (a) and 300 K (b). In black, the corresponding spectra of Powder-1stday are also shown for comparison.

6. EPR spectra for powder sample and for A-, B- and H-type tablets of HKUST-1 reactivated after 5 weeks of aging. ***QUESTO PARAGRAFO E` TUTTO NUOVO***

After 5 weeks of aging the Powder sample has shown some spectroscopic changes (Figure 8). Figure S3 shows EPR measurements obtained at 77 K (a) and 300 K (b) for activated Powder-1stday and for reactivated Powder sample after 5 weeks of aging in the EPR tube. After reactivation (Powder-5weeks-reactivated), the amplitude of the main peak of the spectrum acquired at 77 K has a partial recovery and returns close to that observed in the spectrum acquired for Powder-1stday. Likewise, at 300 K in Figure 4(b) we note a total recovery of the signal after the reactivation, as it has almost the same intensity with respect to that of Powder-1stday. In conclusion, as already reported previously, this heat treatment has a total recovery effect in the aged Powder sample.[39]

Figure S4 shows EPR measurements obtained at 77 K (a) and 300 K (b) for the A-40MPa tablet reactivated 5 weeks after the tableting, compared with those obtained for Powder-1stday. The corresponding comparison has also been made for H2-40MPa tablet and it is shown in Figure S5. Contrary to what was seen for B-40MPa and Powder, in this case A-40MPa-5weeks-Reactivated and H2-40MPa-Reactivated have dissimilar spectra with very different line-shapes, both at 77 K and at

300 K with respect to the Powder sample. In particular, at 300 K (Figure S4(b) and S5(b)), we observe that the spectra are symmetric and now centered at 315 mT, but they are visibly narrower than the Powder sample, with a width of about 70 mT. Furthermore, the A-40MPa-5weeks-Reactivated spectrum has an amplitude at least three times larger than A-40MPa-1stday. Similar remarks apply also to the H2-40MPa sample. Both the spectra of the two tablets obtained at 77 K (Figure S4(b) and S5(b)) show the disappearance of the contributions attributed to the triplet signal, located at 12 mT and 470 mT (Figure 2). At the same time, the central peak changes significantly shape and a new feature having a maximum at about 80 mT appears.

7. XRD patterns and BET analysis

Figure 11 and Figure 12 show the XRD patterns and the N_2 isotherms of the powdered sample (Powder-1stday) and of the samples A-40Mpa e B-40MPa, before and after aging (A-40MPa-1stday, B-40MPa-1stday, A-40MPa-5weeks, B-40MPa-5weeks).

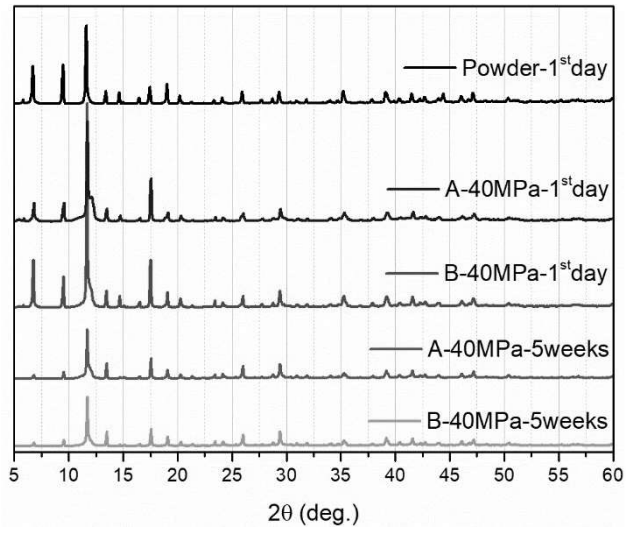

Figure 11. XRD patterns of Powder sample, A-40MPa-1stday, B-40MPa-1stday, A-40MPa-5weeks and B-40MPa-5weeks tablets.

As indicated in Figure 11, the Powder sample can be identified as typical HKUST-1 material possessing Cu-units in paddlewheel conformation arranged through BTC ligands in cubic *Fm-3m* open framework lattice. Compression process does not have significant effect on the overall crystal structure, confirming the rigidity of the Cu-BTC network. Unit cell volume of the sample A-40MPa-1stday decreases by just 0.05% (Table 1) but more significant are the changes in broadening and occurrence of the separate broad peaks near (111) and (222) reflections on the XRD pattern, or rather near the peaks at 5.8° and 11.5° respectively, due to the tetragonal strain of cubic lattice along [111] crystal plane. Such a high-pressure lattice distortion was already predicted by DFT calculations[43] and can be described as a consequence of the deformation of interfacial angles between paddlewheels and interatomic O-$C_{carboxylate}$-C_{phenyl} angles. However, lattice deformation seems to be partially reversibly recovered after subsequent reactivation of the tablets (sample B-40MPa-1stday) indicated by the less pronounced peak broadening in comparison with the sample A-40MPa-1stday. Moreover, unit cell parameters of the sample B-40MPa-1stday become almost identical to the ones of the powdered sample. In both the aged tablets, broadening of the peak at about 11.5°, that is (222) reflections seems to be less pronounced than in fresh tablets, but aging apparently causes a small reduction of the intensity of the peaks below 20° and a slight expansion of the unit cell for 0.3%. The peak at about 14.5° seen in the fresh tablets changes in two smaller peaks in the aged tablets (reflections (331) and (420)). This effect was already observed by Schlichte et al.[3] and it is caused by the presence of water in the lattice.

Table 1. Unit cell parameters.

sample	a (Å)	V (Å^3)
Powder	26.348(2)	18291(4)
A-40MPa-1stday	26.343(6)	18282(12)
A-40MPa-5weeks	26.374(5)	18346(10)
B-40MPa-1stday	26.347(3)	18289(7)
B-40MPa-5weeks	26.371(3)	18338(7)

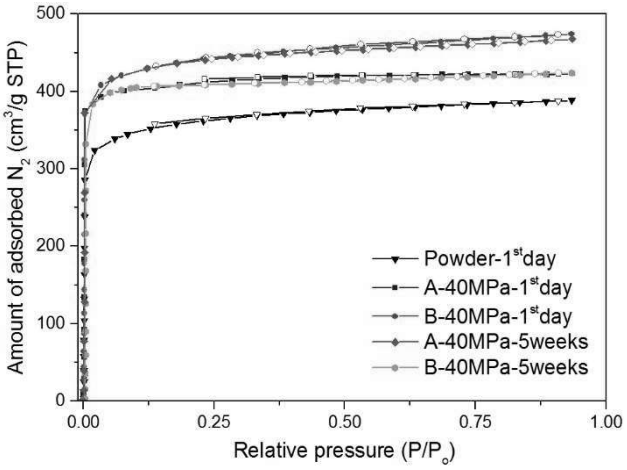

Figure 12. N_2 isotherms of Powder sample, A-40MPa-1stday, B-40MPa-1stday, A-40MPa-5weeks and B-40MPa-5weeks tablets.

N_2 sorption isotherm of all the samples show typical Type I isotherm commonly observed for pure microporous materials with no desorption hysteresis and no increase in N_2 uptake at relative pressures P/P_0 close to 1, indicating the absence of interparticle porosity. The BET surface areas of the samples are shown in Table 2.

Table 2. BET surface area of the Powder sample and some A- and B-type tablets. The analysis was performed in the relative pressure range of the increasing trend of the Rouquerol plot.

sample	BET (m^2/g)
Powder-1stday	1620
A-40MPa-1stday	1685
A-40MPa-5weeks	1848
B-40MPa-1stday	1935
B-40MPa-5weeks	1622

BET surface area of the powdered sample is in the expected range for HKUST-1 powdered materials. Surprisingly, the compression has positive effect on the microporosity which is indicated by the substantial increase of the S_{BET} values to 1685 m^2/g for A-40MPa-1stday and becomes even more significant for the tablet B-40MPa-1stday (S_{BET} = 1935 m^2/g). The aging of the tablet does not affect

the porosity significantly, and the BET surface areas change only for approximately 15% for both the A and B samples. Furthermore, the load capacity of the tablet samples (both as-prepared and aged) is slightly higher than that of the powder sample.

8. Morphological studies, water sorption isotherms, FTIR measurements and thermogravimetric analysis ***QUESTO PARAGRAFO E` TUTTO NUOVO***

Combined optical/AFM studies have been performed in order to gain information on the morphological properties of the investigated samples. In particular, we have deeply investigated the properties of B-type tablet and compared them with those of the pristine powder of HKUST-1. The results are reported in the Supporting Information (Figure S6 – S11) and they clearly show that the B-40MPa tablet actually preserves the main morphology of the pristine material, as it consists of well-packaged grains of HKUST-1. In order to further compare the properties of B-40MPa tablet with those of the Powder sample, water isotherm measurements have been run (Figure S12). Pristine HKUST-1 powder shows typical near type I water isotherm, characterized by two distinctive uptake contributions: the first step is up to relative pressure of 0.25 and it is assigned to the coordination of water on unsaturated Cu^{2+} sites whereas the second step is due to the consecutive filling of the remaining large pore space.[44] Above P/P0 = 0.25 the material achieves saturation. Additional uptake at higher relative pressures (P/P0 > 0.75) is due to the water condensation within the interparticle voids. The significant desorption hysteresis of HKUST-1 powder is a consequence of the strong hydrogen bonding between the cluster of water molecules located within the large hydrophilic pores. Desorption of water does not seem to be completely reversible since the coordinated water is bonded to coordinately unsaturated sites by chemisorption. The water isotherm of the sample B-40MPa shows a similar rapid increase in water uptake at relative pressures P/P0 > 0.15 as in the case of the pristine powder, however the second step is much less pronounced and the water sorption capacity at saturation is lower for approximately 25% if compared with powdered HKUST-1. The change of the

isotherm shape of the tablet indicates that the free Cu^{2+} sites are fully available for the water coordination, on the other hand the filling of the remaining large pore becomes somewhat obstructed. Anyway, desorption is almost completely reversible. Another comparison between the Powder and the B-type tablet has been conducted by the FTIR measurements and it is reported in Figure S13. As shown, the IR spectra of the two samples are virtually indistinguishable between them. Furthermore, they exhibit essentially the same spectroscopic features previously reported in literature for pristine HKUST-1 powder.[23,25,45] Finally, the TGA curves for the A-, B- and H- type samples are compared in Figure S14. These measurements clearly show that the considered samples have a different degree of hydration, which increases in the following order: B-, A-, H2- and H1- sample. All the considered samples have a comparable thermal stability, as they exhibit just minor changes of the temperature of crystal decomposition. Interestingly, smaller temperatures of crystal breakdown are observed for the samples with higher degree of hydration. Furthermore, as it is evident in Figure S14, above the temperature of decomposition the TGA curves obtained for tablets share common features between them, but they differ significantly with respect to those observed for powder samples, suggesting that the decomposition pathway is somewhat different for HKUST-1 in powder and tablet forms.

DISCUSSION

The experimental data reported in Figure 3 concerning H1-40MPa sample prove that 20 minutes of exposure to air on a petri suffice to severely damage the crystal structure of HKUST-1 and to compromise any eventual further treatment as, in our case, tableting. At variance, the EPR spectra of the sample H2-40MPa (Figure 4(a)) indicate that a soft hydration does not compromise the structure of the powders of HKUST-1. However, after tableting of the hydrated powders, both the EPR spectra obtained at 77 K and 300 K undergo relevant changes (Figure 4 (a) and (b)), suggesting that the matrix of HKUST-1 is distorted and/or broken in many sites. Finally, for sake of comparison, we consider

the results reported in Figure 6(a) for the sample A-type compacted with a pressure of 40 MPa. For this latter sample, which consists in a tablet of HKUST-1 obtained from powders not intentionally exposed to air but just rapidly handled in air during the procedure of tableting, the changes induced in the EPR spectra at 77 K and 300 K are significantly reduced with respect to the previous one (H2-40MPa, Figure 4 (a)). Since the sole difference between the latter two samples is the degree of hydration, higher for the former than for the latter, this comparison points out that the water adsorbed on HKUST-1 powders before compaction is one fundamental source of instability of the structure of the material during compaction. In particular, we believe that water molecules may facilitate the distortion and/or the breaking of the lattice during the application of the mechanical pressure to the sample. The distortions may be simply related to steric factors, whereas permanent bond breaking may be due to hydrolyses processes presumably promoted to allow the network to release part of the huge stress induced during compaction of the powders. By TGA measurements we have estimated a number of water molecules adsorbed for Cu^{2+} site of about 3.8, 2.1, 1.0 and 0.67 for the samples H1 powder, H2 powder, A- and B-type tables, respectively (Table S1).

A compatible value of 0.6 has also been obtained for B-40MPa (Table S1) by referring to the water isotherm measurements (Figure S12) and considering that the tableting process takes place at RH=70% and at room temperature. On the basis of these preliminary experimental evidences, we have decided to focus our attention in particular on tablets obtained from dry HKUST-1 powders.

In Figure 6, we have shown the EPR spectra of A-type tablets. In Figure 6(a) in particular, we have noted that the amplitude of the central resonance increases on increasing the applied pressure. This new contribute has some spectral features very similar to that assigned to the paramagnetic centers $[Cu(OH_2)_6]^{2+}$.[33] Therefore, it is reasonable to assume that this additional signal is also due to the spin ½ of Cu^{2+} ions. Considering that the concentration of preexisting $[Cu(OH_2)_6]^{2+}$ complex is a fixed quantity, the increase in intensity of this reasonably involves the decoupling (partial or total) of some Cu^{2+} pairs in a certain number of paddle-wheels of the material. This decoupling may have origin

from a reversible distortion of the paddle-wheels or from some irreversible processes, in which the breakdown of some Cu-O bonds is involved. On the basis of these assumptions and of data in Figure 6(a), we argue that higher is the pressure involved greater is the damage induced in the lattice. Calculating the double integral (DI) of the EPR signal due to S=1/2 species induced by pressure, we have obtained an evaluation of the damage induced to the lattice. We can express these results in terms of spin concentration, for a quantitative estimate of the percentage of damaged paddle-wheels. The outcomes are shown in Figure 13, where we report the percentage of paddle-wheels per unit volume damaged by compaction as a function of the applied pressure. As shown, the amount of broken paddle-wheels increases on increasing the pressure and it reaches the maximum value of only about 4% for a pressure of 40 MPa. Since the powders pressed at 40 MPa show a good mechanical strength (Figure S1) and a very small amount of damaged paddle-wheels, a pressure of 40 MPa represents the best choice for tableting HKUST-1 powder.

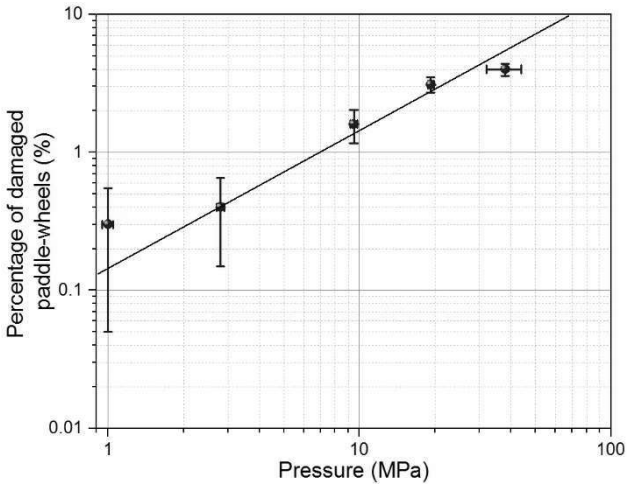

Figure 13. Percentage of damaged paddle-wheels as a function of the applied pressure in logarithmic scale. The traced line has slope of 1.

It is important to underline that the growth of the signal due to the spin S=1/2 centers cannot be easily quantitatively correlated to the decrease of the signal due to the triplet centers present in the spectra obtained at 77 K. In fact, the two species of paramagnetic centers involved, spin 1/2 and interacting spin 1/2 pairs, follow Curie and Bleaney-Bowers laws of magnetic susceptibilities, respectively. The

latter, in particular, is characterized by an exponential functional dependence with respect to the coupling constant J and consequently even small change of the value of J induced by compaction may significantly affect the amplitude of the EPR signal relative to the triplet centers.

The experimental data discussed above make clear that if the starting HKUST-1 in powders form is enough dry and preserved from air moisture, its lattice undergoes only negligible damages when it is subjected to a pressure of 40 MPa. In other words, by preserving the material from air moisture before tableting it is possible to obtain HKUST-1 tablets of great quality, but there is more: reactivating the tablets immediately after tableting, an almost complete recovery of the spectral characteristics of the pristine HKUST-1 powders is observed, as proved by the results obtained for the sample B-40MPa (Figure 7). In particular, the resonance located at about 325 mT at 77 K, whose intensity quantify the damage induced in the crystalline matrix, drastically reduces its amplitude as a consequence of this reactivation. Furthermore, the peaks of the hyperfine structure become again clearly evident (as opposed to sample A-40MPa where they disappeared), indicating a sort of recovery of the pristine structure for most of the paddle-wheels.

In addition, our results indicate that A-type tablets are affected by a gradual spontaneous structural degradation process (Figure 5), whereas these effects are absent in B-type tablets (Figure 10), indicating that the post tableting activation is also capable to prevent this undesired evolution of the sample and consequently to make the tablets stable in time. Again such outcomes suggest the involvement of water molecules as a source of structural instability. In fact, the spontaneous degradation of the crystal of HKUST-1 network after tableting is reasonably related to the release of the residual mechanical stress induced by tableting on the network by hydrolysis of highly strained bonds. This process is probably due to the water molecules adsorbed by the sample during the procedure of tableting, which may be located into the cavities of HKUST-1 or into the interstices between the grains packaged to form the tablet. According to this hypothesis, the reactivation after tableting has the effect to allow the network to release most of the stress induced by compaction and

contemporarily to further release water molecules from the sample. Anyway, it is clear from Figure S4 and S5 that the reactivation has a recovery effect on the properties of the tablets only if it is performed within few hours from the tableting. This picture about B-type samples is in line with the results of XRD, which indicate a reduction of the lattice deformation as a consequence of post-tableting reactivation (Figure 11).

The properties discussed above and obtained mainly on the basis of the study of the magnetic properties of the samples, are also fully supported by the results coming from FTIR measurements and BET analysis. Indeed, the formers point out that the typical frequencies of the network vibrations are not affected by the mechanical compaction, whereas the latter proves that the sample B-40MPa has a value of specific surface that is even better than that of the pristine HKUST-1 powders, a result which mark a new relevant goal in the research field focused on MOF tableting. In addition, we have also experimental evidences of an excellent degree of packaging of the tablets, obtained from the optical/AFM images (Figure S6-S11). Such excellent degree of packaging, while preserving a granular structure similar to that of the pristine material, agree very well with the other results we have found indicating that B-40MPa tablet actually has an effective density comparable with respect to that of the skeleton of HKUST-1, but without a significant damage of the crystalline network. Although the main initial granular structure of the pristine powders of HKUST-1 is preserved in type-B tablet, it is clearly evident both from optical and AFM images that the largest grains are broken in many fragments as a consequence of the tableting process (Figure S6-S11). These effects, together with the spatial reorganization of the grains, presumably helps the system to reach a better level of volume packaging during the application of the pressure.

CONCLUSION

Here we have reported an original experimental investigation on the effects of mechanical compaction on the structure and on the properties of HKUST-1 powders by monitoring the changes induced by

tableting on its magnetic properties by EPR spectroscopy. Thanks to the extraordinary potentialities of this technique in investigating the properties of magnetic materials, we were able to unveil many fundamental properties of the process of tableting of HKUST-1. In particular, we have recognized for the first time that tableting process always induces the growth of S= ½ paramagnetic centers in the materials, whose number increases on increasing the applied pressure. This component derives from the distortion and/or breaking of a fraction of the paddle-wheels of the material, and thus it can be used to obtain a quantitative estimate of the damage induced by compaction in the lattice in correspondence of the metal group. Thanks to this approach, we have unveiled that the number of such defects, and consequently the degree of degradation induced in HKUST-1 upon mechanical compaction, is strictly related to the level of hydration of the starting powders.

In particular, we have estimated that the percentage of paddle-wheels damaged by tableting with a pressure of about 40 MPa is as low as 4% for HKUST-1 tablets obtained from *dry* powders, i.e. containing less than one water molecule adsorbed for Cu^{2+} ion. In addition, we have proved that subjecting the tablets to a further thermal activation just after compaction, this defective EPR component is further drastically reduced and the proprieties of the system becomes virtually indistinguishable with respect to those of activated powders of HKUST-1 with the pristine structure. Furthermore, the same reactivation treatment was found to make the tablet stable in time. All these outcomes are fully supported even by all the other experimental techniques we used in the present work, which are: XRD, N_2 absorption and BET analysis, FTIR, TGA, water sorption isotherms, optical and atomic force (AFM) microscopies.

Summarizing, our results have proved that it is possible to obtain stable tablets of HKUST-1 with the pristine structure by simply taking care to activate the material just before and just after tableting.

SUPPORTING INFORMATION

Additional details about experimental EPR spectra acquired at 300 K and 77 K for aged and reactivated samples, water sorption isotherms, FTIR spectra, TGA measurements, pictures of tablets

and hydrated powders, optical microscopy images and AFM measurements of HKUST-1 in the form of powder and tablet.

ACKNOWLEDGMENT

The authors would like to thank people of the LAMP group (http://www.unipa.it/lamp/) at the Department of Physics and Chemistry of University of Palermo for useful discussions and comments and Prof. G. Lazzara for taking care of some of the thermogravimetric measurements. AFM measurements were performed at the Advanced Technologies Center (http://www.atencenter.com), University of Palermo. Financial support by PJ-RIC-FFABR_2017 is acknowledged.

REFERENCES

(1) Editorial, *Nature Chem.*, 2016, **8**, 987.

(2) Chui, S. S.-Y.; Lo, S. M.-F.; Charmant, J. P. H.; Orpen, A. G.; Williams, I. D. A Chemically Functionalizable Nanoporous Material. *Science* **1999**, *283*, 1148-1150.

(3) Schlichte, K.; Kratzke, T.; Kaskel, S. Improved Synthesis, Thermal Stability and Catalytic Properties of The Metal-Organic Framework Compound $Cu_3(BTC)_2$. *Micropor. Mesopor. Mater.* **2004**, *73*, 81-88.

(4) Xiao, B.; Wheatley, P. S.; Zhao, X.; Fletcher, A. J.; Fox, S.; Rossi, A.G .; Megson, I. L.; Bordiga, S.; Regli, L.; Thomas, K. M., et al. High-Capacity Hydrogen and Nitric Oxide Adsorption and Storage in a Metal-Organic Framework. *J. Am. Chem. Soc*. **2007**, *129*, 1203–1209.

(5) Borfecchia, E.; Maurelli, S.; Gianolio, D.; Groppo, E.; Chiesa, M.; Bonino, F.; Lamberti, C. Insights into Adsorption of NH_3 on HKUST-1 Metal−Organic Framework: A Multitechnique Approach. *J. Phys.Chem. C* **2012**, *116*, 19839−19850.

(6) Nijem, N.; Fürsich, K.; Bluhm, H.; Leone, S. R.; Gilles, M. K. Ammonia Adsorption and Co-Adsorption with Water in HKUST-1: Spectroscopic Evidence for Cooperative Interactions. *J. Phys. Chem. C* **2015**, *119*, 24781−24788.

(7) Lin, K. S.; Adhikari, A. K.; Ku, C. N.; Chiang, C. L.; Kuo, H. Synthesis and Characterization of Porous HKUST-1 Metal Organic Frameworks for Hydrogen Storage. *Int. J. Hydrogen Energ.* **2012**, *37*,13865−13871.

(8) Brown, C. M.; Liu, Y.; Yildirim, T.; Peterson, V. K.; Kepert, C. J. Hydrogen Adsorption in HKUST-1: A Combined Inelastic Neutron Scattering and First-Principles Study. *Nanotechnology* **2009**, *20*, 204025.

(9) Gensterblum, Y. H_2 and CH_4 Sorption on Cu-BTC Metal Organic Frameworks at Pressures up to 15 MPa and Temperatures Between 273 and 318 K. *J. Surf. Eng. Mater. Adv. Technol.* **2011**, *1*, 23−29.

(10) Liu, Y.; Brown, C. M.; Neumann, D. A.; Peterson, V. K.; Kepert,C. J. Inelastic Neutron Scattering of H_2 Adsorbed in HKUST-1. *J. Alloy. Compd.* **2007**, *446*, 385−388.

(11) Getzschmann, J.; Senkovska, I.; Wallacher, D.; Tovar, M.;Fairen-Jimenez, D.; Düren, T.; van Baten, J. M.; Krishna, R.; Kaskel, S. Methane Storage Mechanism in The Metal-Organic Framework $Cu_3[BTC]_2$: An in situ Neutron Diffraction Study. *Micropor. Mesopor. Mater.* **2010**, *136*, 50−58.

(12) Wang, Q. M.; Shen, D.; Bülow, M.; Lau, M. L.; Deng, S.; Fitch, F.R.; Lemcoff, N. O.; Semanscin, J. Metallo-Organic Molecular Sieve for Gas Separation and Purification. *Micropor. Mesopor. Mater.* **2002**, *55*, 217−230.

(13) Li, J. R.; Kuppler, R. J.; Zhou, H. C. Selective Gas Adsorption and Separation in Metal−Organic Frameworks. *Chem. Soc. Rev.* **2009**, *38*, 1477−1504.

(14) Li, J. R.; Ma, Y.; McCarthy, M. C.; Sculley, J.; Yu, J.; Jeong, H. K.; Balbuena, P. B.; Zhou, H. C. Carbon Dioxide Capture-Related Gas Adsorption and Separation in Metal-Organic Frameworks. *Coord. Chem. Rev.* **2011**, *255*, 1791−1823.

(15) J. Ren, B.C.; North, J. Shaping Porous Materials for Hydrogen Storage Applications: A Review. *Technol. Innov. Renew. Energy* **2014**, *3*, 12–20.

(16) Ren, J.,; Langmi, H. W.; North, B. C.; Mathe, M. Review on Processing of Metal–Organic Framework (MOF) Materials Towards System Integration for Hydrogen Storage. *Int. J. Energy Res*. **2015**, *39*, 607–620.

(17) Jia, Z.; Li, H.; Yu, Z.; Wang, P.; Fan, X. Densification of MOF-5 Synthesized at Ambient Temperature for Methane Adsorption. *Mater. Lett*. **2011**, *65*, 2445–2447.

(18) Kim, J.; Kim, S. H.; Yang, S. T.; Ahn, W. S. Bench-Scale Preparation of $Cu_3(BTC)_2$ by Ethanol Reflux: Synthesis Optimization and Adsorption/Catalytic Applications. *Micropor. Mesopor. Mater.* **2012**, *161*, 48-55.

(19) Bazer-Bachi, D.; Assié, L.; Lecocq, V.; Harbuzaru, B.; Falk, V. Towards Industrial Use of Metal-Organic Framework: Impact of Shaping on the MOF Properties. *Powder Technol.* **2014**, *255,* 52–59.

(20) Ardelean, O.; Blanita, G.; Borodi, G.; Lazar, M. D.; Misan, I.; Coldea, I.; Lupu, D. Volumetric Hydrogen Adsorption Capacity of Densified MIL-101 Monoliths. *Int. J. Hydrogen Energ.* **2013**, *38*, 7046–7055.

(21) Nandasiri, M. I.; Jambovane, S. R.; McGrail, B. P.; Schaef, H. T.; Nune, S. K. Adsorption, Separation, and Catalytic Properties of Densified Metal-Organic Frameworks. *Coordin. Chem. Rev.* **2016**, *311*, 38-52.

(22) Dhainaut, J.; Avci-Camur, C.; Troyano, J.; Legrand, A.; Canivet, J.; Imaz, I.; Maspoch, D.; Reinsch H.; Farrusseng, D. Systematic Study of the Impact of MOF Densification into Tablets on Textural and Mechanical Properties. *CrystEngComm* **2017**, *19,* 4211-4218.

(23) Peterson, G.W.; DeCoste, J.B. ; Glover, T.G. ; Huang, Y.; Jasuja, H.; Walton, K.S. Effects of Tableting Pressure on the Physical and Chemical Properties of the Metal–Organic Frameworks $Cu_3(BTC)_2$ and UiO-66. *Micropor. Mesopor. Mat.* **2013***, 179*, 48-53

(24) Finsy, V.; Ma, L.; Alaerts, L.; De Vos, D. E.; Baron, G. V.; Denayer, J. F. M. Separation of CO_2/CH_4 Mixtures with the MIL-53 (Al) Metal–Organic Framework. *Micropor. Mesopor. Mat.* **2009**, *120*, 221–227.

(25) Tian, T., Zeng, Z., Vulpe, D., Casco, M. E., Divitini, G., Midgley, P. A., Silvestre-Albero, J; Tan, J; Moghadam, P. Z.; Fairen-Jimenez, D. A Sol–Gel Monolithic Metal–Organic Framework with Enhanced Methane Uptake. *Nat. mater.* **2018**, 17(2), 174.

(26) Gascon, J.; Aguado, S.; Kapteijn, F. Manufacture of Dense Coatings of $Cu_3(BTC)_2$ (HKUST-1) on α-Alumina. *Micropor. Mesopor. Mat.* **2008**, *113*, 132.

(27) Akhtar, F.; Andersson, L.; Ogunwumi, S.; Hedin, N.; Bergström, L.; Structuring Adsorbents and Catalysts by Processing of Porous Powders. *Eur. Ceram. Soc.* **2014**, *34*, 1643–1666.

(28) Zacher, D.; Shekhah, O.; Wöll, C.; Fischer, R. A. Thin Films of Metal–Organic Frameworks. *Chem. Soc. Rev.* **2009**, *38*, 1418–1429.

(29) Tian, T.; Velazquez-Garcia, J.; Bennett, T. D.; Fairen-Jimenez, D. Mechanically and Chemically Robust ZIF-8 Monoliths with High Volumetric Adsorption Capacity. *J. Mater. Chem. A* **2015**, *3*, 2999–3005.

(30) Liu, J.; Thallapally, P. K.; Strachan, D. Metal–Organic Frameworks for Removal of Xe and Kr from Nuclear Fuel Reprocessing Plants. *Langmuir* **2012**, *28,* 11584-11589.

(31) Ahmed, A.; Forster, M.; Clowes, R.; Myers, P.; Zhang, H. Hierarchical Porous Metal–Organic Framework Monoliths. *Chem. Commun.* **2014**, *50,* 14314-14316.

(32) Prestipino, C.; Regli, L.; Vitillo, J. G.; Bonino, F.; Damin, A.; Lamberti, C.; Zecchina, A.; Solari, P. L.; Kongshaug, K. O.; Bordiga, S. Local Structure of Framework Cu(II) in HKUST-1 Metallorganic Framework: Spectroscopic Characterization Upon Activation and Interaction with Adsorbates. *Chem. Mater*. **2006**, *18*, 1337−1346.

(33) Pöppl, A.; Kunz, S.; Himsl, D.; Hartmann, M. CW and Pulsed ESR Spectroscopy of Cupric Ions in the Metal−Organic Framework Compound $Cu_3(BTC)_2$. *J. Phys. Chem. C* **2008**, *112*, 2678-2684.

(34) Zhang, X. X.; Chui, S. S.-Y.; Williams, I. D. Cooperative Magnetic Behavior in the Coordination Polymers $[Cu_3(TMA)_2L_3]$ (L=H2O, pyridine). *J. Appl. Phys*. **2000**, *87*, 6007-6009.

(35) Rodríguez-Fortea, A.; Alemany, P.; Alvarez, S.; Ruiz, E. Exchange Coupling in Carboxylato-Bridged Dinuclear Copper(II) Compounds: A Density Functional Study. *Chem. - Eur. J.* **2001**, *7*, 627−637.

(36) Agnello, S.; Boscaino, R.; Cannas, M.; Gelardi, F. M. Instantaneous Diffusion Effect on Spin-Echo Decay: Experimental Investigation by Spectral Selective Excitation. *Phys. Rev. B: Condens. Matter Mater. Phys.* **2001**, 64, 174423.

(37) Šimėnas, M.; Kobalz, M.; Mendt, M.; Eckold, P.; Krautscheid,H.; Banys, J.; Pöppl, A. Synthesis, Structure, and Electron Paramagnetic Resonance Study of a Mixed Valent Metal−Organic Framework Containing Cu_2 Paddle-Wheel Units. *J. Phys. Chem. C* **2015**, 119, 4898−4907.

(38) El Mkami, H.; Mohideen, M. I. H.; Pal, C.; McKinlay, A.;Scheimann, O.; Morris, R. E. EPR and Magnetic Studies of a Novel Copper Metal Organic Framework (STAM-I). *Chem. Phys. Lett.* **2012**, *544*, 17−21.

(39) Todaro, M., Buscarino, G., Sciortino, L., Alessi, A., Messina, F., Taddei, M., Ranocchiari, M., Cannas, M. and Gelardi, F.M. Decomposition Process of Carboxylate MOF HKUST-1 Unveiled at the Atomic Scale Level. *J. Phys. Chem. C*, **2016** *120*, 12879-12889.

(40) Bleaney, B.; Bowers, K. D. Anomalous Paramagnetism of Copper Acetate. *Proc. R. Soc. Lond. A* **1952**, *214*, 451−465.

(41) Wasserman, E.; Snyder, L. C.; Yager, W. A. ESR of the Triplet States of Randomly Oriented Molecules. *J. Chem. Phys.* **1964**, *41*, 1763−1772.

(42) Perec, M.; Baggio, R.; Sartoris, R. P.; Santana, R. C.; Peña, O.;Calvo, R. Magnetism and Structure in Chains of Copper Dinuclear Paddlewheel Units. *Inorg. Chem.* **2010**, *49*, 695−703.

(43) Wu, H.; Yildirim, T.; Zhou, W. Exceptional Mechanical Stability of Highly Porous Zirconium Metal–Organic Framework UiO-66 and its Important Implications. *Phys.Chem. Lett.* **2013**, *4*, 925.

(44) Küsgens, P., Rose, M., Senkovska, I., Fröde, H., Henschel, A., Siegle, S., Kaskel, S. Characterization of Metal-Organic Frameworks by Water Adsorption. *Micropor. Mesopor. Mat.* **2009** 120(3), 325-330.

(45) Dhumal, N. R., Singh, M. P., Anderson, J. A., Kiefer, J., Kim, H. J. Molecular Interactions of a Cu-Based Metal–Organic Framework with a Confined Imidazolium-Based Ionic Liquid: a Combined Density Functional Theory and Experimental Vibrational Spectroscopy Study. *J. Phys. Chem. C* **2015** 120(6), 3295-3304.

TOC Graphic

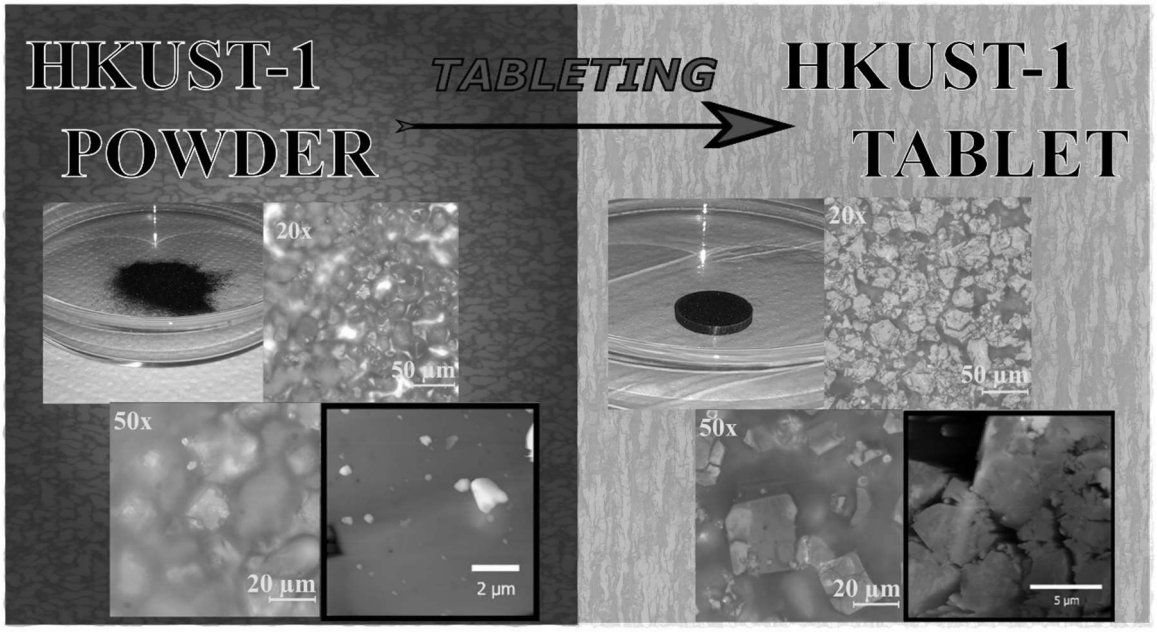
HKUST-1
POWDER
TABLETING
HKUST-1
TABLET
20x
50 µm
50x
20 µm
2 µm
20x
50 µm
50x
20 µm
5 µm